ERDC/CERL SR-12-15

Construction Engineering
Research Laboratory

US Army Corps
of Engineers®
Engineer Research and
Development Center

Energy Balance Calculations for an Anaerobic Membrane Bioreactor

Carl A. Feickert, Kathryn Guy, and Martin Page

December 2012

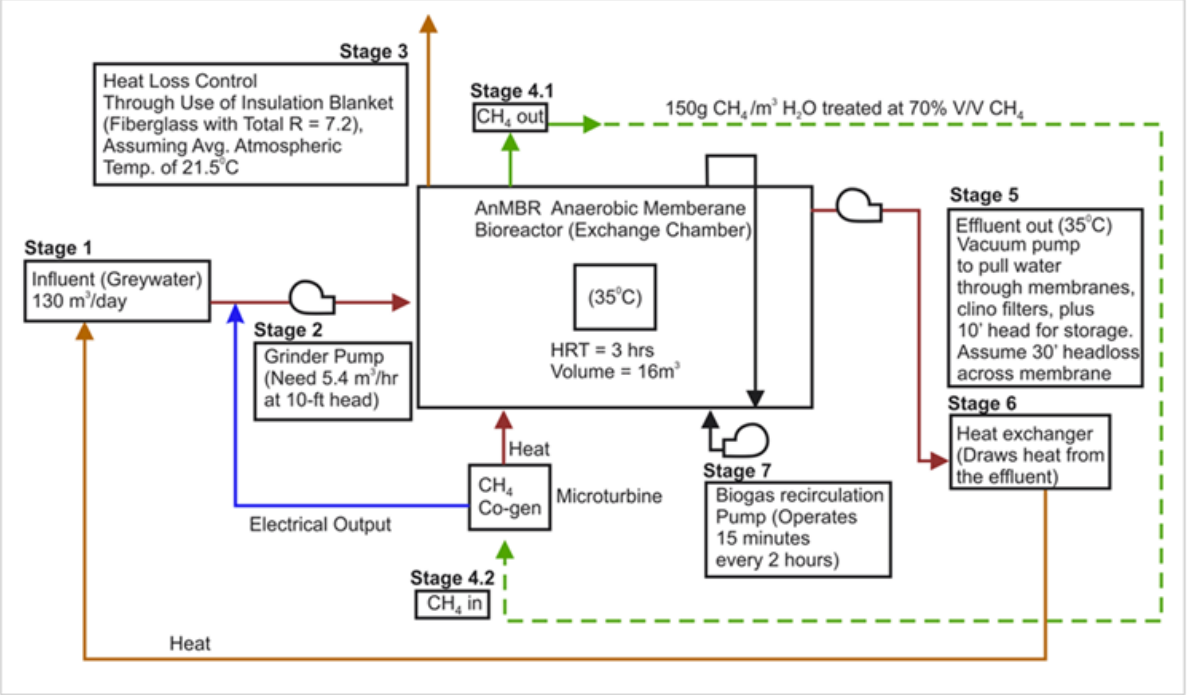

ERDC/CERL SR-12-15
December 2012

Energy Balance Calculations for an Anaerobic Membrane Bioreactor

Carl A. Feickert, Kathryn Guy, and Martin Page

Construction Engineering Research Laboratory (CERL)
US Army Engineer Research and Development Center
2902 Newmark Dr.
Champaign, IL 61822-1076

Final Report

Prepared for Headquarters, US Army Corps of Engineers
Washington, DC 20314-1000

Abstract

For the Army of the 21st Century, energy and water have become premium resources that must be conserved. Wastewater treatment plants (WWTPs) at both domestic installations and forward operating bases are net users of energy. Energy costs can account for 30% of the total operation and maintenance costs of WWTPs. Further secondary treatment processes for the removal of organic matter and nitrogen based compounds including ammonia account for 60% of a WWTP's energy consumption. A new research effort described here, employing an anaerobic membrane bioreactor (AnMBR) technology, will offer a more efficient method for the removal of organics. Ammonia in the AnMBR effluent will be subsequently treated using novel methods, replacing current energy intensive treatments options. This report has delineated the flow of energy through the AnMBR system as a preliminary and necessary step to assess the integrated system's design and efficiency.

Table of Contents

Preface

This study was conducted for the Strategic Environmental Research and Development Program (SERDP) Office under a project titled "Novel Anaerobic Wastewater Treatment Systems for Energy Generation at Forward Operating Bases," led by Dr. Kathryn Guy. The technical reviewers were Dr. Kathryn Guy and Dr. Martin Page, CEERD-CF-M.

This work was managed by the Materials Branch (CF-M) of the Facilities Division (CF), Construction Engineering Research Laboratory, US Army Engineer Research and Development Command (CERL-ERDC). The ERDC-CERL Principal Investigator (PI) was Dr. Kathryn Guy, CEERD-CF-E. At the time of publication, Franklin H. Holcomb was Chief, CEERD-CF-E. and L. Michael Golish was Chief, CEERD-CF. The associated Technical Director was Martin J. Savoie, CEERD-CVT. The Deputy Director of ERDC-CERL was Dr. Kirankumar V. Topudurti and the Director was Dr. Ilker R. Adiguzel.

The Commander and Executive Director of ERDC is COL Kevin J. Wilson, and the Director of ERDC is Dr. Jeffery P. Holland.

1 Introduction

Background

The development of sustainable wastewater treatment solutions has been identified as an important area of research for domestic installations and forward operating bases (FOBs) (Noblis 2010). The treatment of wastewater on-site with minimal energy and chemical inputs will reduce the logistical burdens and costs associated with the transportation of materials to and from FOBs. The availability of treated water for reuse will further decrease this burden as water and fuel combine to account for a large majority of supply shipments in Afghanistan and Iraq (Noblis 2010). Sustainable wastewater systems that fit within the constraints of FOB operations and that can be incorporated into larger net-zero energy design schemes reduce costs while improving security and environmental stewardship.

Conventional wastewater treatment relies heavily on activated sludge processes for secondary treatment, in which removal of organics and other oxygen-demanding constituents is a primary goal. The aeration required to support this process represents a major energy cost- typically more than half of the total energy used for wastewater treatment (Wallis-Lage and Levesque 2009). In pursuit of more energy-efficient approaches to wastewater treatment, researchers have proposed that anaerobic membrane reactor technology (AnMBR) be applied to a greater extent as an alternative to aerobic activated sludge processes.

AnMBR technology can be applied to degrade organics in wastewater and generate methane, which can be harvested for thermal energy. Although anaerobic treatment schemes have been studied for decades, AnMBRs are still considered embryonic technologies (Berube et al. 2006; USEPA 2008). AnMBRs have been demonstrated to reduce chemical oxygen demand (COD) by 90% in synthetic wastewater with influent COD values of 460 mg/L, at hydraulic retention times (HRTs) greater than 3 hr, and the AMBRs produced in excess of 0.25 m^3 methane per kg COD removed from municipal wastewater, at a methane gas concentration of 70% (Hu and Stuckey 2006). With careful attention to reactor design, they can be made highly efficient in terms of physical footprint and operational stability. Key enabling technologies for AnMBRs include hydrophilic, foulant-resistant

membranes and strategies for reducing scale formation on the membrane surface (Hu and Stuckey 2006, Choo et al. 2000).

The Engineer Research and Development Center, Construction Engineering Research Laboratory (ERDC-CERL) is exploring the details of AnMBR design as part of a larger research effort leading to reduced energy consumption and conservation of water for secondary reuse. A major factor in the overall AnMBR design efficiency is a careful accounting for how energy is used and produced during the reactor operation. This report sets forth and details some of the energy calculations required for this assessment, and a first order explanation of some of the physical (power, energy, chemical) features that must be considered in the integrated design and development of such systems.

Objectives

The objective of this work was to delineate and assess the flow of energy through a system that incorporates AnMBR to remove organic matter and particulates from wastewater.

Approach

This objective of this stage of work was accomplished through primary research based on literature survey and first order engineering calculations that rely on basic physics and chemistry, conservation of energy, and practical engineering knowledge and experience regarding the general efficiency of rotational pumps, and internal combustion engines for conversion of chemical energy into power.

Scope

Energy balance methods employed in this assessment rely on basic physics and chemistry, conservation of energy, and practical knowledge regarding the general efficiency of rotational pumps, and internal combustion engines for conversion of chemical energy into power. These calculations are first order in accuracy and are not implied to represent detailed (10% or better) engineering calculations. However, they should be considered accurate at the 20% level (most probably better).

Mode of technology transfer

This report will be made accessible through the World Wide Web (WWW) at URLs:

http://www.cecer.army.mil

http://libweb.erdc.usace.army.mil

2 Underlying Assumptions

The AnMBR process

Figure 1 shows a diagram of a generic AnMBR with supporting pumps, heating/heat exchange systems, and waste bio-gas recycling apparatus. In the figure, numerical labels identify individual components for easy reference throughout this document. This assessment considers both fluid and energy flows together at each stage since the fluid is the medium used to generate and transport the major energy flows in and out of the reactor.

Throughout this analysis, the incoming wastewater and exiting wastewater from the reactor are assumed to have the density, heat capacity, and viscosity equal to that of clear water at 77 °F (25 °C). During actual operation, the wastewater will contain dissolved salts, chemicals, and organic particulates; however, the clear water assumption is considered accurate for the required level of accuracy. Other components such as piping and reactor construction details have stated values.

The calculations that follow also depend on an assumption that all power consumption (or production) for the entire system (volume flow-through rate, temperature, and gas emissions) is derived from a continuous steady state (24/7) operating condition, i.e., the system is *not* operated in a "batch" mode. Given this assumption, the design parameters for the AnMBR system are:

- A 1000-person FOB generates 130 m^3 of wastewater per day.
- The self contained AnMBR is capable of processing this wastewater at the required rate, with a 3-hour hydraulic retenton time (HRT).
- Wastewater is assumed to enter the reactor system at 21 ˚C, to undergo a preheating to 35 ˚C, and to be maintained at 35 ˚C during the HRT and on exiting the system. An external heat/heat exchange system, with attendant pumping capability is required to maintain the reactor's 35 ˚C temperature during the continuous operation.
- Waste stream heat and gaseous emissions are to be recovered so far as practical and reused so as to conserve overall energy requirements.

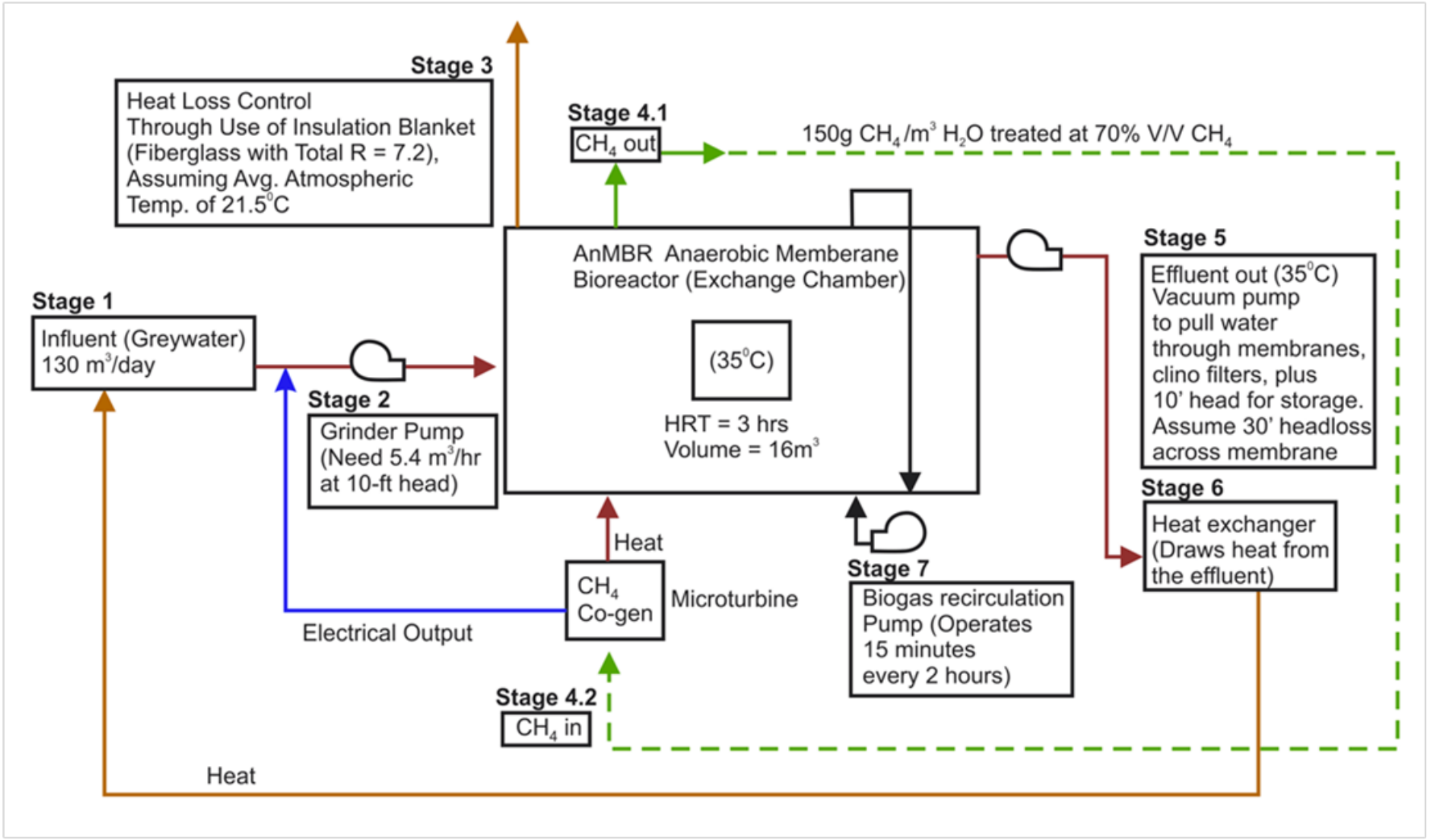

Figure 1. Generic anaerobic bioreactor process flow with the following constraints: @25 °C, COD = 1g/L, and NH_3 has a concentration of 5mM.

Construction details

The construction and design of the actual bioreactor will depend on certain parameters. The bioreactor has an HRT of 3 hours and a design volume of ~16.25 m^3. To contain this volume in a rectangular shaped reactor, one can assume dimensions of: height = 2.84 m, width = 1.42 m, and length = 4.05 m. Adding the ~8.06 m^2 area of the two ends to the ~34.5 m^2 lateral area gives a combined total surface area of ~42.6 m^2. This value will be used later in the report for more detailed surface energy transfer loss calculations.

In addition, it is desirable to have an estimate of the weight of the bioreactor. Apart from its surface volume, the reactor contains two internal baffles having individual areas ~75% that of the end plate area (2*75%*4.05 m^2, = 6.05 m^2), which makes for a combined total surface area of ~48.7 m^2. The total volume of material is then estimated as the reactor's wall thickness times total area. To ensure sufficient structural strength, the reactor's wall thickness was (conservatively) chosen at 0.25-in. steel (0.635 cm). Assuming a density of steel at ~7.9 grams/cm^3, the total weight is then:

$$\sim(7.9 \text{ grams/cm}^3)*48.7*(100 \text{ cm})^2*(0.635 \text{ cm}) = \sim 2443 \text{ kg}$$

The initial theoretical energy required to heat this much *steel* (wastewater, not included) from 21˚C to the operating temperature of 35˚C is found by using a specific heat of iron (~3.54 J/[cm^3 - °C]), the change in reactor temperature, and the previously computed steel volume. This then will require an initial heating energy input of:

$$3.54 \text{ J/[cm}^3\text{- °C]}*(35\text{-}21 \text{ ˚C})*48.7*(100 \text{ cm})^2*(0.635 \text{ cm}) = \sim 15.1*10^6 \text{ J}$$

Having reached this temperature, the design operating conditions will maintain the bioreactor's temperature through normal operations such that no further energy is required.

3 Energy Flow Calculations

Stage 1

Given these assumptions and parameters outlined in Chapter 2 (130-m^3/day volume flow), the *continuous flow-through rate* (volume/second) for the bioreactor is:

130-m^3/day*1000 L/m^3*day/(24*3600 s) = 1.505 L/s

The size of the bioreactor with an HRT of 3 hours is then:

(3*3600-s/HRT)*1.505 L/s = 16,254 L or ~16.25 m^3

From the flow rate and the requirements of incoming and preheated change in wastewater temperature, one can compute the rate of energy (power) required to heat the water prior to entering the reactor. Using a specific heat of water of 4.18 J/(cm^3 °C), the power (at Stage 1, assuming 100% heating efficiency) is then:

Power (heating) = 14 °C*4.18 J/(cm^3 °C)*1505cm^3/sec = ~88.05 kW

This power can be delivered by a resistive wire-wound heat exchanger element in close contact with the cooler incoming reactor water, or by some sort of secondary heat recovery systems such as a heat exchanger.

Stage 2

Continuing to the grinder-pump (Stage 2), this pump must be capable of providing sufficient power to work against the hydraulic head, estimated at 10 ft of water, and to puree the typical organic matter found in a wastewater stream. This grinding action will add to the typical inefficiency of a normal hydraulic pump and will be *approximated* as an additional loss of around 10 to 15% of that required by the pumping of pure water. In a traditional hydraulic pumping scenario, there is no internal energy change to the water from the pumping action as the specific heat of the water is treated as that of an incompressible fluid. Also a reasonable pump pipe diameter of ~2 in. will reduce the power associated with taking stationary water and accelerating it to the design flow rate into the reactor.

Other loss mechanisms such as friction loss in pipes and at right-angle bends can also be shown negligible to the same level. The power required to pump water at the design flow rate and hydraulic head is therefore:

$$\text{Pump Power} = P_{hydro} * (\text{Flow rate}) \quad (1)$$

A 10-ft hydraulic head has a Pressure (P_{hydro}) of:

$$P_{hydro} = (10\ \text{ft} * 12 * 2.54\text{cm/ft}) * (1\text{-kg}/[1000\text{cm}^3]) * 9.8\text{m/sec}^2$$
$$.= \sim 2.98\ \text{N/cm}^2$$

Thus at the required continuous flow rate, the grinder-pump will consume (per Equation 1):

$$(2.98\ \text{N/cm}^2) * 1.505\ \text{L/s} = \sim 4.48 * \text{L/s} * (1000\ \text{cm}^3/\text{L}) * \text{N/cm}^2 = 44.8\ \text{W}$$

This value is for a perfectly efficient pump. Since typical hydraulic mechanical pumps operate at efficiencies of ~66% and one assumes an additional 10% loss for the grinding process, the grinder-pump at Stage 2 will require approximately:

$$\text{Stage 2 Pump Power} = \sim 44.8\ \text{W}/(.66 - .10) = \sim 80.3\ \text{W}$$

Stage 3

At Stage 3, one has a relatively warm reactor vessel at 35 ˚C surrounded by the relatively cooler ambient temperature of 21 ˚C. Thermally conductive pathways to the ground can be a source of significant heat loss, but depend on the details of the reactor's foundation support. For this theoretical assessment, they remain undefined; however, a more refined engineering design must address this heat loss.

Two other additional heat loss paths are known: Black Body radiation losses and convective air film thermal transport. If one considers just the warm uninsulated metallic walls of the reactor exposed to ambient temperature, it can be shown that these two heat loss mechanisms are significant and comparable in size. For reference, the power loss through Black Body (B.B.) radiation in a vacuum is:

$$\text{B.B.-Power/Area} = \varepsilon\sigma T^4$$

where:

σ = 5.67×10^{-8} W m^{-2} K^{-4} the Stefan–Boltzmann constant
T is the (reactor) temperature in absolute degrees Kelvin
ε is the emissivity, a unitless constant dependent on the surface properties.

However, the reactor is not in a vacuum, but is immersed in the ambient thermal bath; as such, it receives energy back from the environment. Assuming the emissivity of air is ~1, one can show (Bird 1965) that the B.B. Power/area loss of the uncovered warm reactor in the parallel plane limit is:

$$\text{B.B.-Power/area} = \varepsilon\sigma[\,(273+35)^4 - (273+21)^4\,] \quad (2)$$

For oxidized iron ε = ~0.8, so that B.B. power loss to the ambient air from the warm reactor is ~68.5 W/m^2.

For the case of convective heat loss (from the air) around the warm unshielded reactor, Langmuir (Anderson 1989) derived a result for the heat transfer from a (warmer) vertical surface at temperature T_2 to the ambient air at temperature T_1 as:

$$\text{Convective Power/area} = 93{,}000(\phi_2 - \phi_1)\ \text{W/m}^2 \quad (3)$$

The ϕ_j's are given in tabular form as a function of T in absolute Kelvin for $0 < T_j <$ ~520 °K, and can be represented as:

$$\phi_j = T_j\,(-4.169*10^{-11}*T_j^2 + 1.232*10^{-7}*T_j - 2.562*10^{-6})$$

This formulation gives comparable results to similar treatments found in the literature (Bird 1965). Inserting the values of 35 ˚C for the reactor and 21 ˚C for the ambient air temperature, one finds that the convective heat loss for the unshielded reactor is ~78.5 W/m^2. For a corresponding horizontal surface, these results can differ by some 10 to 50% depending on thermal orientation of the surface relative to air flow. However unlike the B.B. results, convective heat transfer is relatively insensitive to surface properties or structure. In these types of formulations, the heat transfer depends explicitly on the physical properties of the air, such as density, thermal conductivity, specific heat, and viscosity. Collectively, these two mechanisms could result in a loss of ~147 W/m^2 for the unshielded reactor

surface. For a reactor of ~42 m^2 of surface area (see construction details above) this amount (in Stage 3) is a combined loss of:

> Surface Power loss of ~6.2 kW to the air from the reactor's uninsulated surface.

Both B.B. and convective loss mechanisms can be attenuated by the application of a surface insulation to the reactor. The application of an insulating layer reduces the surface heat flux and temperature to a value such that the surface B.B. and convective heat loss is able to balance and remove the attenuated heat flux passing through and leaving the insulation-air interface. A rigorous treatment of heat transport requires that these two coupled mechanisms be dealt with in a self-consistent manner, both at the reactor's surface and at the external surface of the insulating material. For the purpose of this study, the exact solution will be approximated by appealing to the underlying physics. The ideal situation is to be able to design a practical insulating material and thickness such that the external surface temperature of the insulation is as close to the ambient air temperature as possible (21 ˚C for this assessment).

For the design of insulated shielded surfaces, a traditional insulation metric is the "R-value" of an insulating material. The R-value defines the heat flux for a given temperature difference across a slab of insulation of thickness, δ, as:

$$\text{Power Loss through Insulation/Area} = (T_{hot} - T_{cool}) / (\delta R), \quad (4)$$

where R has mixed (Imperial, SI) units of: (˚C/in.)/(W/m^2).

Thus increasing the insulation's thickness from 1 to 2 in. reduces the transmitted power by a factor of two. Typical R-values of fiberglass or polystyrene foam have R-values = 0.5 to 0.7/in. (Johns Manville Insulation 2012). Using the design temperature and parameters of:

- $T_{hot} - T_{cool}$ = 13.5 ˚C, corresponding to a 21.5 ˚C surface temperature
- a 12-in thickness of R = 0.6 foam or fiber glass (total R = 7.2)
- a surface emissivity, ε = 0.4 which is characteristic of aluminum paint.

Equation 4 predicts a thermal flux across the external (21.5 ˚C) insulated surface, of ~1.9 W/m^2. By contrast, the B.B. radiation flux (Equation 2) for this (21.5 ˚C) surface temperature is only ~1.14 W/m^2, which would suggest

a slightly higher surface temperature required for radiation energy balance. However for the 21.5 ˚C surface temperature, the convective power loss is already at ~2.8 W/m^2, which requires the surface to be at some temperature less than 21.5 ˚C for energy balance. Hence (Stage 3), a 12 in. thickness of R = 0.6 foam (total R = 7.2) is adequate for a reasonable exterior temperature (~21 °C).

Finally, using the above exterior area information, one concludes that (disregarding the ground conductive loss through any of the reactor's support structures) this amount of insulation will reduce the original total ~6.2 kW heat loss to ~80 W.

Stage 4

At Stages 4.1 and 4.2, the primary issue is the recovery of waste methane gas from the bioreactor and its possible use as an energy source. Several options are available:

- Burn the methane gas to preheat the incoming water.
- At Stage 4.2, remove hydrogen sulfide from the methane waste stream, internally reform the methane, and then use the resulting hydrogen gas in a fuel cell system.
- Straight methane combustion in a diesel engine to provide shaft power for an electric generator.

The second option (Stage 4.2) requires very large amounts of waste gas, to be energetically cost effective in a fuel cell system capable of generating mega watts of power. For the system under review here, the fuel cell is not a realistic option because of the large energy requirements to reform and clean the methane (Josefik and Swanson). A diesel generator is much more tolerant to the presence of H_2S in the fuel stream and is a straightforward viable option for the combustion of the methane in conjunction with a heat exchanger. Also, the diesel electric generator unit is a mature technology with many off-the-shelf options available.

The design parameter for Stage 4.1 indicate the production of 150 grams of methane per cubic meter of processed wastewater. At a steady state flow of ~1.505 L/sec this requires 1000 L/(1.505 L/s) = 664.5 seconds for the 150 grams of methane, or 0.226 grams/second. If one assigns a lower heating value (through combustion [Bolz and Tuve 1973]) of ~50 k Joules/gram of

methane, then pure methane combustion liberates ~11.3 kW of thermal power at the specified flow rates. Continuing, using the methane as fuel for a diesel-electrical generator one finds that typical electrical generators about ~90 to 95% efficient, and that typically diesel generators are ~35% efficient in turning fuel energy into rotational power. Hence of the original 11.3 kW, one might expect to recover by use of a diesel generator system:

3.4 to 3.8 kW of electrical power from methane combustion

The remaining balance (~7.9 to 7.5 kW) of the original 11.3 kW derived from methane combustion is lost as waste heat in the exhaust stream. However, if this heat were to be captured with a heat exchanger, it could then be made available to preheat the incoming Stage-1 cool water, thereby offsetting some of the initial water heating requirements. Finally, if the 0.226 grams/second of methane are burnt directly in a heat exchanger, one might expect to recover somewhat more than 3.6 kW of thermal heating value, depending on the details of the heat exchange unit (see "Stage 6" below).

Stage 5

At Stage 5, a vacuum pump is used to pull reactor discharge water through a filter membrane with 30 ft of head loss and against an additional hydraulic head of 10 ft, for a total equivalent hydraulic head of 40 ft at the steady state flow design flow rate. Assuming all the relevant conditions and efficiency of the Stage-2 pump, but *excluding* the 10% grinder power loss, the power required at Stage-5 is four times that found at Stage 2 for the pure hydraulic case:

Stage 5 Pump Power = ~275 W

Stage 6

Stage 6 represents recovery of some of the heat contained in the reactor's discharge water and can amount to a significant contribution to the overall system energy balance if captured with a heat exchanger. Typically a heat exchanger can have fixed input temperatures for fluids at the incoming "Hot" and "Cold" sides of the exchanger. However, the temperatures of the fluids on the exiting side of the exchanger are parametric variables that depend on flow rates (in and out) as well the details of the exchanger's construction. A simple heat exchange model can be used to provide guidance as how best to adjust overall heat transfer as a function of these par-

ametric variables. Figure 2 schematically shows the fundamental variables required for the model.

The heat exchanger can be thought of as two straight pipes, which are thermally connected and containing fluid flowing in opposite directions so as to increase the transfer efficiency. Let the pipes be of equal length L, carrying fluids with specific heat capacity C_i (energy per unit mass per unit change in temperature) and let the mass flow rate of the fluids through the pipes be $\hat{m}_i$ (mass per unit time), where the subscript i applies to Pipe 1 or Pipe 2. Let $T_{2,0}$ and $T_{1,0}$ be the temperatures at x=0 and let $T_{2,L}$ and $T_{1,L}$ be the temperatures at the end of the pipe at x=L. These temperatures serve as the state variables for the system, with the incoming hot fluid, $T_{2,L}$ and cold fluid $T_{1,0}$ considered constants of the system. The exiting fluids $T_{1,L}$ and $T_{2,0}$ are considered parametric variables to be optimized for the particular system requirements.

The temperature profiles for the pipes are $T_1(x)$ and $T_2(x)$ where x is the distance along the pipe. For this model, one assumes a steady state flow so that the temperature profiles are not functions of time along the individual pipes, and that the only transfer of heat is from a small volume of fluid in one pipe to a corresponding fluid element in the adjacent pipe at the same location.

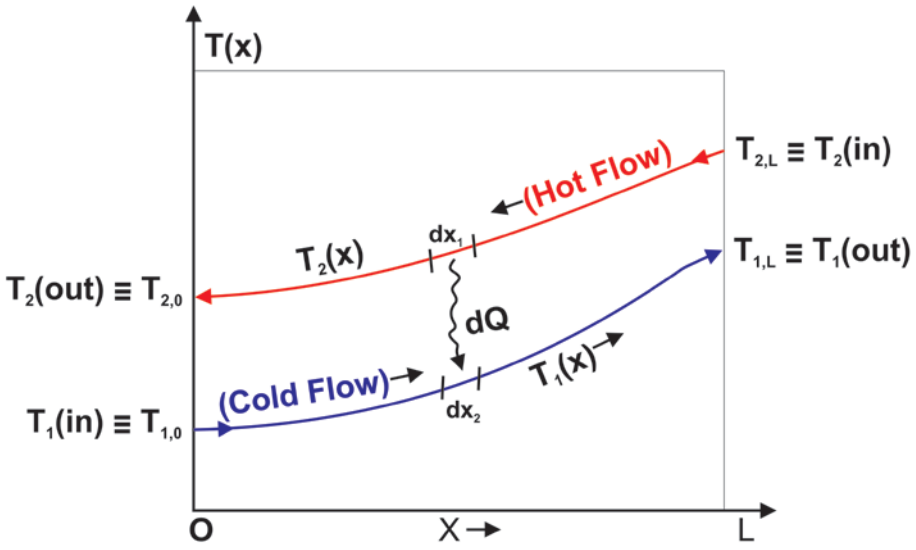

Figure 2. Thermal and spatial coordinate variables used for a 1-D generic heat exchange model. Horizontal axis, x, defines the spatial coordinate and vertical axes is used to depict spatial variation of temperature, T(x), for incoming hot and cold fluids.

Further, because of the steady state nature of the flow, there will be no transfer of heat *along* a pipe due to local temperature differences within that pipe. Although this is not strictly true, this first order approximation is in keeping with a model having no second order spatial derivatives of the temperature. Then the rate of change in energy for a small volume of fluid (within the pipe) is proportional to the difference in temperatures between it and the corresponding element in the adjacent pipe:

$$\frac{du_1}{dt} = \gamma\left(T_2 - T_1\right), \text{ and } \frac{du_2}{dt} = \gamma\left(T_1 - T_2\right) \tag{5}$$

where:

$u_i(x)$ is the thermal energy transferred or received per unit length between the pipes

γ is the thermal connection constant per unit length between the two pipes, and is dependent on the geometry and material composition of the pipes.

For precision of the model, consider a concentric two-pipe heat exchanger, fashioned from copper and having a common wall thickness of δt, which separates the fluids. Then $\boldsymbol{\gamma}$ is:

$$\gamma = \frac{K_{Cu} D\pi f}{\delta t}, \text{ [units of, W/(cm-°C)]} \tag{6}$$

where:

K_{Cu} is the thermal conductivity of copper (W/cm-°C).

$D\pi$ represents the length of the common boarder through which heat flows. For this explicit case, it is the cross sectional circumference of the interior pipe of diameter D.

f is a dimensionless efficiency factor that takes into account the fact that not all of the fluid in Pipes 1 and 2 have equal access to the surface where heat exchange will take place during their residency time in the exchanger. The choice of its value depends critically upon the constructions details of the heat exchanger, circulation and turbulence flow considerations.

Further this transfer of internal energy per unit length between pipes, results in a temperature change of the individual fluid elements located along the pipes. The time rate of change for the fluid energy per unit length carried along by the flow is:

$$\frac{du_1}{dt} = J_1 \frac{dT_1}{dx}, \text{ and } \frac{du_2}{dt} = J_2 \frac{dT_2}{dx} \tag{7}$$

where: $J_i = C_i \ \hat{m}_i$ is the "thermal mass flow rate" (W/°C).

The differential equations governing the heat exchanger may now be written as:

$$J_1 \frac{\partial T_1}{\partial x} = \gamma\left(T_2 - T_1\right), \text{ and } J_2 \frac{\partial T_2}{\partial x} = \gamma\left(T_1 - T_2\right) \tag{8}$$

Note that since the system is in a steady state, there are no partial derivatives of temperature with respect to time, and since there is no heat transfer (*assumed*) along the pipe, there is no second derivative in x as found in the heat equation. Using the definition of the $J_i = C_i \ \hat{m}_i$, one has that:

$\hat{m}_1 = \frac{dm_1}{dt}$ is the mass flow rate of water to be heated and is equal to 1-kg/L times the volume flow rate, which in this instance is 1.505 L/s, and similarly for $\frac{dm_2}{dt}$, the water to be cooled in the heat exchanger

Here both flow rates are assumed to be free variables, not necessarily equal. The C_j are the individual specific heat capacities of the fluids flowing through the heat exchanger (assumed to be water and identical). For water the C_j's are equal to: 4.185 J/g-K.

Continuing, Equations 8 can be collectively solved for the temperature profiles of $T_1(x)$ and $T_2(x)$ along the pipes, in terms of the constants J_i and **γ.** The resulting solutions are simple constants and exponentials having x-functionality. Using these solutions and Equations 5 and 7, one can then show that the total rate of energy transferred is found by integrating the expressions for the time rate of change of internal energy per unit length:

$$\frac{dU_1}{dt} = \int_0^L \frac{du_1}{dt} dx = J_1\left(T_{1,L} - T_{1,0}\right) = \gamma L\left(\overline{T}_2 - \overline{T}_1\right)$$

and: (9)

$$\frac{dU_2}{dt} = \int_0^L \frac{du_2}{dt} dx = J_2\left(T_{2,L} - T_{2,0}\right) = \gamma L\left(\overline{T}_1 - \overline{T}_2\right)$$

Here it is useful to define the following average temperatures along the individual heat exchanger pipes as:

$$\overline{T}_1 = \frac{1}{L}\int_0^L T_1(x)dx \text{, and } \overline{T}_2 = \frac{1}{L}\int_0^L T_2(x)dx \quad (10)$$

Both sets of Equations 9 for the total rate of energy transferred, can be couched in terms of the previously defined state variables, and the term $\overline{T}_2 - \overline{T}_1$. By using the general solutions for $T_1(x)$ and $T_2(x)$, one can also show that $\overline{T}_2 - \overline{T}_1$ can also be expressed in terms of the state variables as:

$$\overline{T}_2 - \overline{T}_1 = \frac{\left(T_{2,L} - T_{1,L}\right) - \left(T_{2,0} - T_{1,0}\right)}{\ln\left(\frac{T_{2,0} - T_{1,0}}{T_{2,L} - T_{1,L}}\right)} \quad (11)$$

The quantity $\overline{T}_2 - \overline{T}_1$ is known as the "log mean temperature difference" in the literature, and is an important measure of the effectiveness of the heat exchanger in transferring heat energy. In this analysis, it will also be known as the "thermal power factor" since by Equations 9 it controls the thermal power flow between the fluids exchanging heat. By the conservation of energy, the sum of the two energies in Equations 9 must be zero. Using the explicit results of Equations 11 and 6, one can now attempt to model some of the power recovered (transferred to the fluid in Tube 1) from a heat exchanger using the first of Equations 9:

$$\frac{dU_1}{dt} = \gamma L(\overline{T}_2 - \overline{T}_1) \quad (12)$$

Consider a heat exchanger with the following design input parameters:

- Incoming hot fluid, $T_{2,L}$ = 35 ˚C.
- Incoming cold fluid $T_{1,0}$ = 21 ˚C.
- The length, L, of the heat exchanger = 1.2 m.
- The thermal conductivity of copper walled pipes = ~4.01 W/(cm-˚C).
- An internal pipe diameter, D = 4 cm (for the coaxial pipe system), with a common wall thickness of δt, which separates the two fluids = ~0.3 cm.
- A f value, for the dimensionless efficiency factor, conservatively chosen to be 0.50.

Then by Equation 6, Equation 12 (for the transfer of recoverable heat to the cooler fluid) becomes:

$$\frac{dU_1}{dt} = 10.08^*(\bar{T}_2 - \bar{T}_1), \text{[units of, kW]} \quad (13)$$

The quantity $\bar{T}_2 - \bar{T}_1$ is not unique, but depends on the parametric values of the exiting fluids $T_{1,L}$ and $T_{2,0}$ that must be chosen so as to optimize a given system. This may best be done by creating a series of level plots of $\bar{T}_2 - \bar{T}_1$ as a function of the cooler exit fluid temperature, $T_{1,L}$, and using the warmer exit fluid temperature, $T_{2,0}$, as a control variable (Figure 2). Using Equation 11 and the design input parameters to Equation 13 results in the chart shown in Figure 3.

A characteristic of such a level plot is the fact that maximum *power* will be transferred when $T_{1,L} = \sim T_{1,0}$ and $T_{2,L} = \sim T_{2,0}$. Physically, in this limit, there is negligible temperature variation along the pipes so that an overall maximum $(\bar{T}_2 - \bar{T}_1)$ is obtained with corresponding power transferred. This then requires the cool $T_{1,0}$ and warm $T_{2,L}$ fluids to enter the exchanger with large flow rates so as to maintain approximately constant values of $T_1(x)$ and $T_2(x)$ along the entire length.

Examination of the individual level plots verifies this physical concept, since for a given $T_{1,L}$ the value of $(\bar{T}_2 - \bar{T}_1)$ increases monotonically with increasing choice of the control variable $T_{2,0}$, and *decreasing* choice of the free variable $T_{1,L}$. The choice of level curve is completed by specifying the hot water exit temperature, $T_{2,0}$, which is defined by the manufacture or choice of high temperature water flow rate. The model further assumes an ideal thermal transfer efficiency unencumbered by pipe fouling and is limited only by the physics of real world heat transfer.

Another constraint on the operational envelope for the model heat exchanger is available by use of the first set of Equations 9 where $(\bar{T}_2 - \bar{T}_1)$ is related to the free variable by $(T_{1,L} - T_{1,0})$. One can use the design parameters of Equations 13, the specific heat of water (4.185 J/g-K) and the Pipe 1 flow rate, V [in L/sec @ T_{10}] treated as a parametric variable, to provide an alternative constraint on the $(\bar{T}_2 - \bar{T}_1)$ parameter as follows:

$$(\bar{T}_2 - \bar{T}_1) = (J_1/\gamma L)(T_{1,L} - T_{1,0}) = 0.4153V(T_{1,L} - 21\,^{\circ}\text{C}) \quad (14)$$

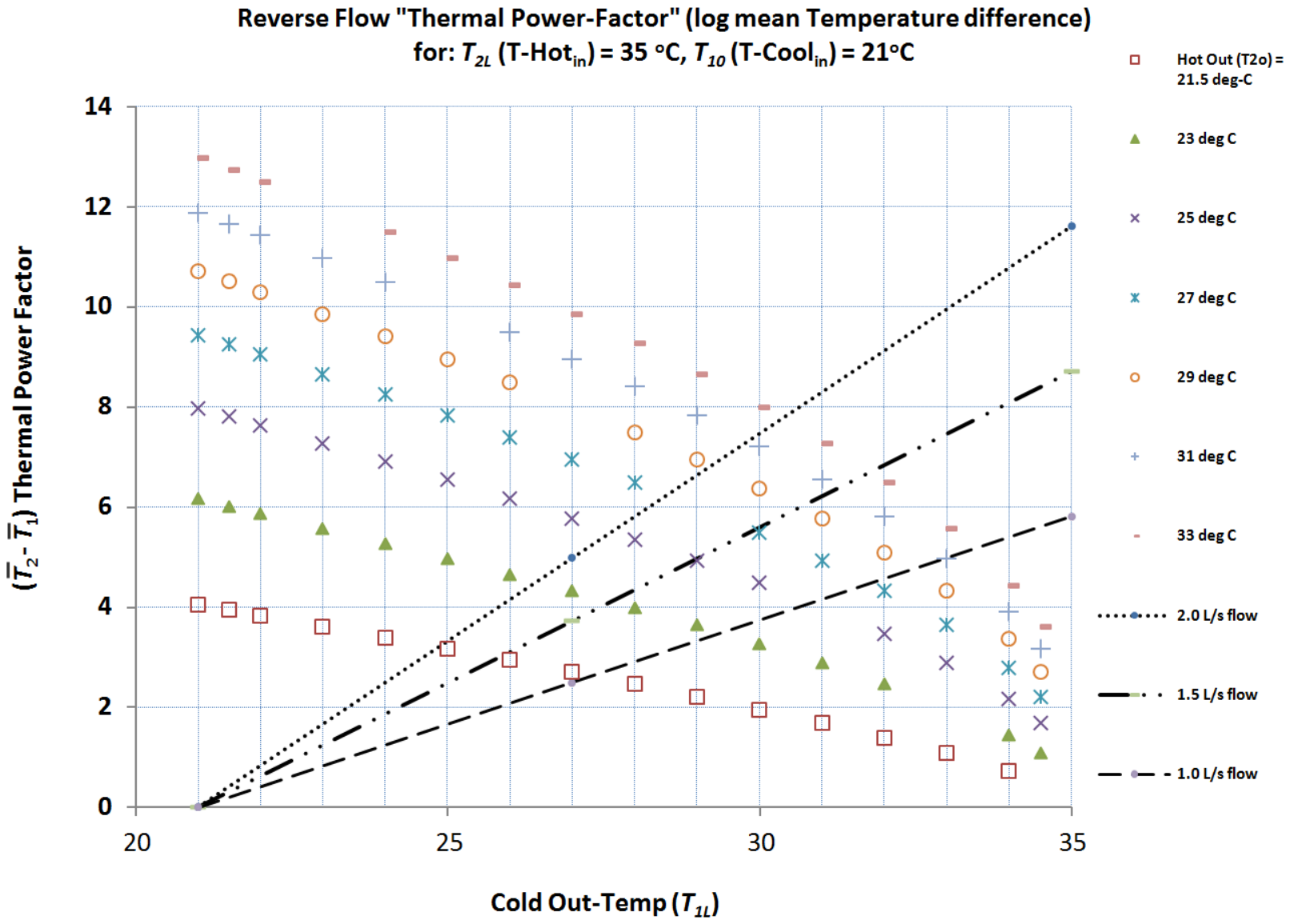

Figure 3. Level plots of $\overline{T}_2 - \overline{T}_1$ as a function of the cooler exit fluid temperature, $T_{1,L}$, and using the warmer exit fluid temperature, $T_{2,0}$, as a control variable.

Returning to Figure 3, Equation 14 is shown as the straight line features for three separate characteristic cold water flow rates into the reactor (2.0 L/s, 1.5 L/s and 1 L/s). For a *given choice* of thermal power factor ($\overline{T}_2 - \overline{T}_1$) and exit hot water temperature, $T_{2,0}$, a corresponding value of the cooler fluid exit temperature, $T_{1,L}$, is then defined depending on flow rate (V) though Pipe 1. This flow rate is functionality imbedded in the slope parameter of Equation 14, ($J_1/\boldsymbol{\gamma}L$), and increases with increasing flow rate. Hence, for a given ($\overline{T}_2 - \overline{T}_1$) factor, a larger flow will imply a lower exit temperature, $T_{1,L}$, due to a reduced residency time with in the exchanger. Similarly if the thermal connection constant, $\boldsymbol{\gamma}$, is reduced perhaps due to pipe fouling, the ($J_1/\boldsymbol{\gamma}L$) ratio is also increased with a corresponding reduction in heat transfer and exit pipe temperature of the fluid being warmed.

Taken collectively, the intersection of a particular line with a level curve then defines the value of exit temperature, $T_{1,L}$, for the water being warmed and the value of the corresponding thermal power factor ($\overline{T}_2 - \overline{T}_1$). For example, if one uses the design flow rate for the cooler water into the reactor of ~1.5 L/sec, then choosing a hot water exit temperature of, $T_{2,0}$ = 33 ˚C, yields a cold fluid exit temperature, $T_{1,L}$ = ~31.8 ˚C. The corresponding thermal power factor ($\overline{T}_2 - \overline{T}_1$) is equal to ~6.7 ˚C and implies by Equation 13 that ~67 kW of water reheating power can be recovered through the heat exchanger at Stage 6.

Similarly for this input flow, choosing a hot water exit temperature of, $T_{2,0}$ = 23 ˚C, yields a cold fluid exit temperature, $T_{1,L}$ = ~27.5 ˚C, with a corresponding thermal power factor, ($\overline{T}_2 - \overline{T}_1$), equal to ~4.0 ˚C. The heating power recovered in this instance is only ~40 kW. Finally, other analysis options are possible, for example specifying all the state variables: $T_{2,0}$, $T_{1,0}$, $T_{2,L}$, and $T_{1,L}$ and then using the available heating power as defined by Equations 9 and 11.

Note that the forgoing analysis is general and does not require equal flow rates for hot and cold fluids. The original design requirements assume a continuous flow processing system, such that the input and output flows are equal. Figure 3 suggests however, that a faster flow of hot water can provide a larger heat transfer power factor. Such a faster flow can be accomplished by using narrower pipes with corresponding smaller contact areas, or a larger pump power that enables increased flow rates.

Another option could be to intermittently capture and retain the hot water leaving the bioreactor for later use at the higher flow rates. This approach will require additional plumbing, thermally insulated retention tanks, pumps and control strategies, all of which will increase the cost, complexity and maintenance of such a bioreactor remediation facility.

Stage 7

For the Stage 7 "bubbler pump," because of the intermittent 15-minute operation every 2 hours, one can assume an equivalent continuous power consumption of ~10-15W.

4 Conclusion

This work has delineated and assessed some of the energy balance considerations required of an AnMBR system, so as to be capable of efficiently removing organics from the effluent wastewater of a typical FOB. The calculated values for the various stages shown on Figure 1 (p 5) are specific to a given geometry and flow rate and illustrate the particular options defined by the original design parameters.

Nevertheless, many other options may be available, particularly with the heat recovery from fluids in the hydraulic heat exchanger. Additional calculations may provide better guidance, so as to optimize the AnMBR system for greater energy efficiency and water conservation, once the details of flow rates, geometry, materials choices, and chemical reactions are know with greater precision.

Acronyms and Abbreviations

Term	Definition
AnMBR	Anaerobic Membrane Reactor (Technology)
ASCE	American Society of Civil Engineers
CEERD	US Army Corps of Engineers, Engineer Research and Development Center
CERL	Construction Engineering Research Laboratory
COD	Chemical Oxygen Demand
DC	District of Columbia
USEPA	US Environmental Protection Agency
ERDC	Engineer Research and Development Center
FOB	Forward Operating Base
HRT	Hydraulic Retention Time
MBR	Membrane Bioreactor
OMB	Office of Management and Budget
PI	Principal Investigator
SERDP	Strategic Environmental Research and Development Program
SF	Standard Form
SI	Systeme Internationale
SR	Special Report
USEPA	US Environmental Protection Agency
WWW	World Wide Web

References

Anderson, Herbert L. (ed.). 1989. *A physicist desk reference*. 2d ed. New York, NY: American Institute of Physics.

Bérubé, P. R., E. R. Hall, and P. M. Sutton. 2006. "Parameters governing permeate flux in an anaerobic membrane bioreactor treating low-strength municipal wastewaters: A literature review." *Water Environment Research 78(8)*:887-896.

Bird, R. B., W. E. Stewart, and E. N. Lightfoot. 1965. *Transport Phenomena*. New York, NY: John Wiley & Sons.

Bolz, Ray E., and George L. Tuve (eds.). 1973. *Handbook of Tables for Applied Engineering Science*. Cleveland, OH: CRC Press.

Choo, K. H., I. J. Kang, S. H. Yoon, H. Park, J. H. Kim, S. Adiya, and C. H. Lee. 2000. "Approaches to membrane fouling control in anaerobic membrane bioreactors." *Water Science and Technology* 41(10):363-371.

Hu, A. Y., and D. C. Stuckey. 2006. "Treatment of dilute wastewaters using a novel submerged anaerobic membrane bioreactor." *Journal of Environmental Engineering* 132(2):190-198.

Johns Manville Insulation. 2012. *Wall insulation*. Web page. Accessed 25 September 2012, http://www.jminsulation.com.au/products/

Josefik, Nicholas, and Matthew Swanson. 2012. Personal communication.

Noblis. 2010. *SERDP Report on Sustainable Forward Operating Bases*.

SBW Consulting, Inc. 2002. *Energy Benchmarking Secondary Wastewater Treatment and Ultraviolet Disinfection Processes at Various Municipal Wastewater Treatment Facilities*. San Francisco, CA: Pacific Gas and Electric Company, http://www.cee1.org/ind/mot-sys/ww/pge2.pdf

US Environmental Protection Agency (USEPA). February 2008. *Emerging Technologies for Wastewater Treatment and In-Plant Wet Weather Management*. EPA 832-R-06-006. Washington, DC: USEPA Office of Wastewater Management.

Wallis-Lage, C. L. and S. D. Levesque. 2009. *Cost Effective & Energy Efficient MBR Systems*. Web page. Accessed 5 January 2010, http://www.bvwater.com

REPORT DOCUMENTATION PAGE

Form Approved
OMB No. 0704-0188

1. REPORT DATE (DD-MM-YYYY)	2. REPORT TYPE	3. DATES COVERED (From - To)
21-12-2012	Final	

4. TITLE AND SUBTITLE
Energy Balance Calculations for an Anaerobic Membrane Bioreactor

5a. CONTRACT NUMBER

5b. GRANT NUMBER

5c. PROGRAM ELEMENT

6. AUTHOR(S)
Carl A. Feickert, Kathryn Guy, and Martin Page

5d. PROJECT NUMBER
SERDP

5e. TASK NUMBER

5f. WORK UNIT NUMBER

7. PERFORMING ORGANIZATION NAME(S) AND ADDRESS(ES)
US Army Engineer Research and Development Center (ERDC)
Construction Engineering Research Laboratory (CERL)
PO Box 9005,
Champaign, IL 61826-9005

8. PERFORMING ORGANIZATION REPORT NUMBER
ERDC/CERL SR-12-15

9. SPONSORING/MONITORING AGENCY NAME(S) AND ADDRESS(ES)
US Army Engineer Research and Development Center (ERDC)
Construction Engineering Research Laboratory (CERL)
PO Box 9005
Champaing, IL 61826-9005

10. SPONSOR/MONITOR'S ACRONYM(S)
CEERD-CF-M

11. SPONSOR/MONITOR'S REPORT NUMBER(S)

12. DISTRIBUTION/AVAILABILITY STATEME
Approved for public release; distribution is unlimited.

13. SUPPLEMENTARY NOTES

14. ABSTRACT

For the Army of the 21st Century, energy and water have become premium resources that must be conserved. Wastewater treatment plants (WWTPs) at both domestic installations and forward operating bases are net users of energy. Energy costs can account for 30% of the total operation and maintenance costs of WWTPs. Further secondary treatment processes for the removal of organic matter and nitrogen based compounds including ammonia account for 60% of a WWTP's energy consumption. A new research effort described here, employing an anaerobic membrane bioreactor (AnMBR) technology, will offer a more efficient method for the removal of organics. Ammonia in the AnMBR effluent will be subsequently treated using novel methods, replacing current energy intensive treatments options. This report has delineated the flow of energy through the AnMBR system as a preliminary and necessary step to assess the integrated system's design and efficiency.

15. SUBJECT TERMS
wastewater treatment plant (WWTP), energy efficiency, bioreactor, power generation

16. SECURITY CLASSIFICATION OF:			17. LIMITATION OF ABSTRACT	18. NUMBER OF PAGES	19a. NAME OF RESPONSIBLE PERSON
a. REPORT	b. ABSTRACT	c. THIS PAGE			19b. TELEPHONE NUMBER (include area code)
Unclassified	Unclassified	Unclassified	SAR	30	